Journal of Hazardous Materials 185 (2011) 447–455

Contents lists available at ScienceDirect

Journal of Hazardous Materials

journal homepage: www.elsevier.com/locate/jhazmat

Adsorption characteristics of UO_2^{2+} and Th^{4+} ions from simulated radioactive solutions onto chitosan/clinoptilolite sorbents

Doina Humelnicu[a,*], Maria Valentina Dinu[b], Ecaterina Stela Drăgan[b]

[a] "Al. I. Cuza" University of Iasi, Faculty of Chemistry, Bd. 11 Carol I, 700506 Iasi, Romania
[b] "Petru Poni" Institute of Macromolecular Chemistry, Aleea Grigore Ghica Voda 41A, 700487 Iasi, Romania

ARTICLE INFO

Article history:
Received 9 June 2010
Received in revised form 1 September 2010
Accepted 16 September 2010
Available online 22 September 2010

Keywords:
Chitosan
Clinoptilolite
Composite
Radiocations
Sorption

ABSTRACT

Adsorption features of UO_2^{2+} and Th^{4+} ions from simulated radioactive solutions onto a novel chitosan/clinoptilolite (CS/CPL) composite as beads have been investigated compared with chitosan cross-linked with epichlorohydrin. The effects of contact time, the initial metal ion concentration, sorbent mass and temperature on the adsorption capacity of the CS-based sorbents were investigated. The adsorption kinetics was well described by the pseudo-second order equation, and the adsorption isotherms were better fitted by the Sips model. The maximum experimental adsorption capacities were 328.32 mg Th^{4+}/g composite, and 408.62 mg UO_2^{2+}/g composite. The overall adsorption tendency of CS/CPL composite toward UO_2^{2+} and Th^{4+} radiocations in the presence of Cu^{2+}, Fe^{2+} and Al^{3+}, under competitive conditions, followed the order: $Cu^{2+} > UO_2^{2+} > Fe^{2+} > Al^{3+}$, and $Cu^{2+} > Th^{4+} > Fe^{2+} > Al^{3+}$, respectively. The negative values of Gibbs free energy of adsorption indicated the spontaneity of the adsorption of radioactive ions on both the CS/CPL composite and the cross-linked CS. The desorption level of UO_2^{2+} from the composite CS/CPL, by using 0.1 M Na_2CO_3, was around 92%, and that of Th^{4+} ions, performed by 0.1 M HCl, was around 85%, both values being higher than the desorption level of radiocations from the cross-linked CS, which were 89% and 83%, respectively.

1. Introduction

Removal of radioactive ions from the wastewaters is a huge problem because these ions are extremely dangerous for the environment and human health by their high toxicity even at very low concentrations and long half lives. These pollutants arise into the wastewaters as a result of different industrial activities like: mining, production of nuclear fuels, laboratory investigations, etc. The methods developed for the removal of radioisotopes from the wastewaters include: chemical precipitation, ion exchange, membrane-related processes, biological processes and electrochemical techniques [1–3]. Because of some disadvantages, which these techniques have (time-consuming processes, high costs, sometimes other toxic wastes are generated) other novel techniques have been developed. Sorption of heavy and radioactive metal ions from effluents proved to be very efficient, numerous sorbents being used for the removal of uranium and thorium from the wastewaters, such as: natural and modified clays [4,5], microorganisms [6], activated carbon [7], different types of cellulosic materials [8], zeolites [9,10], etc. Clinoptilolite (CPL), one of the most common natural zeolites, is a hydrated alumina-silicate member of the heulandite group, occurring in the zeolitic volcanic tuffs, being widespread in many countries in the world. CPL is characterized by infinite three-dimensional frameworks of $[AlO_4]^{5-}$ and $[SiO_4]^{4-}$ tetrahedra linked to each other by sharing all the oxygen atoms, the negative charge being balanced by metal cations, like Na^+, K^+, Ca^{2+}, Mg^{2+} [11]. Its adsorption capacity for heavy metal cations and organic pollutants has been demonstrated [11–14].

Natural polymeric materials have attracted considerable interest for removal of heavy metals due to their biodegradability and non-toxic nature. Among biopolymers, chitosan (CS) is a linear cationic polysaccharide composed of β-(1→4)-2-amino-2-deoxy-D-glucopyranose and β-(1→4)-2-acetamido-2-deoxy-D-glucopyranose units, randomly distributed along the polymer chain, being widely used as biosorbent in wastewater remediation [15,16]. To improve the mechanical properties, adsorption capacity, or even to prevent dissolution in acidic medium of the CS, numerous studies have been devoted to the chemical modification of CS by homogeneous or heterogeneous cross-linking with di- or polyfunctional agents, such as sodium tripolyphosphate, glutaraldehyde, ethyleneglycol diglycidyl ether and epichlorohydrin [15–19]. On the other hand, CS based composite materials have also been reported to exhibit enhanced mechanical, thermal or adsorption properties comparative with any of its components used alone.

* Corresponding author. Tel.: +40232201136; fax: +40232201313.
E-mail addresses: doinah@uaic.ro (D. Humelnicu), vdinu@icmpp.ro (M.V. Dinu), sdragan@icmpp.ro (E.S. Drăgan).

0304-3894/$ – see front matter © 2010 Elsevier B.V. All rights reserved.
doi:10.1016/j.jhazmat.2010.09.053

In this context, we have recently reported on the synthesis of some novel CS/CPL composites by embedding zeolite microparticles in a matrix of cross-linked CS [20,21]. The influence of different parameters like: pH, contact time, temperature, metal ion concentration on the adsorption capacity of the CS/CPL composites against three environmentally problematic divalent metal ions, namely, Cu^{2+}, Co^{2+} and Ni^{2+}, from aqueous solutions, have been examined. The maximum adsorption capacity was found to be 11.32 mmol Cu^{2+}/g, 7.94 mmol Ni^{2+}/g and 4.209 mmol Co^{2+}/g for CS/CPL composites containing 20 wt.% of zeolite, at pH 5 [22]. Therefore, we have now extended the investigations to the adsorption performance of the above-mentioned CS/CPL composite against two radioactive ions, namely, UO_2^{2+} and Th^{4+}, by batch adsorption technique. The influence of experimental conditions, such as contact time, initial metal ions concentration, sorbent mass, and temperature on the adsorption features was studied and compared with cross-linked CS. The Freundlich, Langmuir and Sips equations were used to fit experimental data of the equilibrium isotherm. The adsorption rates were determined quantitatively and compared by pseudo-first and pseudo-second order models and intra-particle diffusion model.

2. Materials and methods

2.1. Chemicals

CS as powder was purchased from Fluka, ash content less than 1%, and was used without further purification. The viscometric average molar mass and the deacetylation degree of CS used in this study were 334 kDa and 82.4%, respectively. These values were estimated according to the methods previously presented [21]. The natural CPL sample used in the preparation of the composite comes from volcanic tuffs containing 60–70% CPL, cropped out in Macicas area (Cluj County, Romania), and has the following elemental composition: $(NaKCa_{0.5})_{5.4}(Al_{5.4}Si_{30.6}O_{72})\cdot 20H_2O$ (Si/Al = 5.7) [11]. The zeolitic volcanic tuff was used as collected. $UO_2(NO_3)_2\cdot 6H_2O$ and $Th(NO_3)_4\cdot 4H_2O$ were used as radiocations source for the adsorption experiments. All the reagents were of analytical grade or highest purity available, and used without further purification. Distilled water was used to prepare all solutions.

2.2. Preparation and characterization of CS/CPL composite microspheres

The CS/CPL composite was prepared as microspheres by a "tandem" ionic/covalent cross-linking, according to the method previously presented [21]. The CS solution, with a concentration of 3 wt.%, was obtained by dissolving the CS powder in 1 vol.% acetic acid solution and intensive stirring for at least 48 h. Typically, 20 g of CS solution (containing 0.6 g CS) were mixed with 10 mL of distilled water containing 0.15 g CPL powder, and after a vigorous magnetic stirring (one hour at least), the epichlorohydrin (ECH) as cross-linker (0.54 mL) was added step-by-step. The mixing went on until the ECH was completely included in the reaction mixture. The mass ratio between CS and CPL in the case of this synthesis was 4:1. The mixture thus prepared was added by a syringe into 180 mL aqueous solution of sodium tripolyphosphate (TPP) with a concentration of 0.05 M, under mild magnetic stirring. The composite microspheres were kept under stirring 5 h at 37 °C, and then were separated from the dispersion medium and washed with distilled water. After that, the wet composite microspheres were treated with a solution of sodium hydroxide 0.1 N and were kept under stirring 2 h at 37 °C to improve their mechanical properties in dry state. Then, the wet microspheres were collected and extensively rinsed with deionized water until neutral pH was reached. For characterization in dried state, the composite microspheres were filtered off, dried at room temperature for 24 h and under vacuum at 40 °C, for 48 h.

The ionic composite CS/CPL was characterized by environmental scanning electron miscroscopy (ESEM), X-ray diffraction (XRD) and Fourier transform infrared spectroscopy (FTIR). The ESEM characterization was performed on samples fixed by means of colloidal silver on copper supports. The samples were covered with a thin layer of gold by sputtering (EMITECH K550X). The coated surface was examined by using the Environmental Scanning Electron Microscope type Quanta 200, operating at 15 kV with secondary electrons, in high vacuum mode. XRD was performed on a Diffractometer Bruker D8 ADVANCE, Bragg-Brentano parafocusing goniometer, scans recorded in step mode by using the Ni-filtered Cu-Kα radiation (λ = 0.1541 nm). The working conditions were 36 kV and 30 mA tube power. The diffractograms were collected in the range of 5–40°, 2θ, at room temperature. The fine powders were obtained in a ball mill pulverizer, in liquid nitrogen. Bruker computer softs "Eva 11" and "Topaz 3.1" were used to process and plot the data. FTIR spectra were recorded with a Bruker Vertex FT-IR spectrometer, resolution 2 cm^{-1}, in the range of 4000–400 cm^{-1} by KBr pellet technique, the amount of the sample being 3 mg in each pellet.

Point of zero charge (PZC) of the cross-linked CS and CS/CPL composite as fine powder was determined by the potentiometric titration by using the particle charge detector PCD 03, Mütek GmbH, Herrsching, Germany. The surface charge density was determined by colloidal titration, with the same equipment, by using an aqueous solution of poly(sodium ethylenesulfonate) with a concentration of 10^{-3} mol/L.

2.3. Sorption experiments

Stock radioactive simulated solutions were prepared by adding the corresponding amount of $UO_2(NO_3)_2\cdot 6H_2O$ and $Th(NO_3)_4\cdot 4H_2O$ in distilled water, after some drops of HNO_3 have been added. The solutions with different concentrations of UO_2^{2+} and Th^{4+} ions were obtained by subsequent dilution of stock solution. As a source for competitive cations in the sorption process, the following salts have been used: $FeSO_4\cdot 7H_2O$, $CuSO_4\cdot 5H_2O$, $Al_2(SO_4)_3$, all from Merck, prepared with the same concentrations like UO_2^{2+} and Th^{4+} solutions. All experiments were performed in duplicate and averaged values were taken and all results represent measurements with an estimated standard deviation of 5%. Solution pH was 4.0, or 5.5 in the case of UO_2^{2+} and Th^{4+}, respectively, being controlled by a buffer solution of CH_3COOH/CH_3COONa [23,24]. The concentration of metal ion varied in the range 10–100 mg/L, temperature in the range 293.15–333.15 K, contact time varied in the range 60–360 min, and sorbent amount 0.01–0.04 g.

After the adsorption tests, the sorbent particles have been filtered off and the concentration of radioactive ions has been spectrophotometrically determined with Arsenazo III. The absorbances of the complexes formed between radioisotopes and Arsenazo III have been measured by the spectrophotometer CECIL 1020, at the characteristic wavelengths of the complexes (665 nm for UO_2^{2+}, and 660 nm for Th^{4+}) [25,26]. The concentration of competitive cations has been measured by PerkinElmer Analyst 200 atomic absorption spectrometer (wavelengths for Cu – 324.7 nm, Fe – 248.3 nm, and Al – 309.3 nm).

Distribution coefficient, K_d, is used to describe the sorption process of metal ions [27]. The distribution coefficient (K_d) was calculated with Eq. (1):

$$K_d\,(\mathrm{mL/g}) = \frac{C_i - C_e}{C_e}\frac{V}{m}, \tag{1}$$

where m – the mass of solid phase (g); V – volume of UO_2^{2+} or Th^{4+} solution in contact with sorbent (mL); C_i – initial concentration of

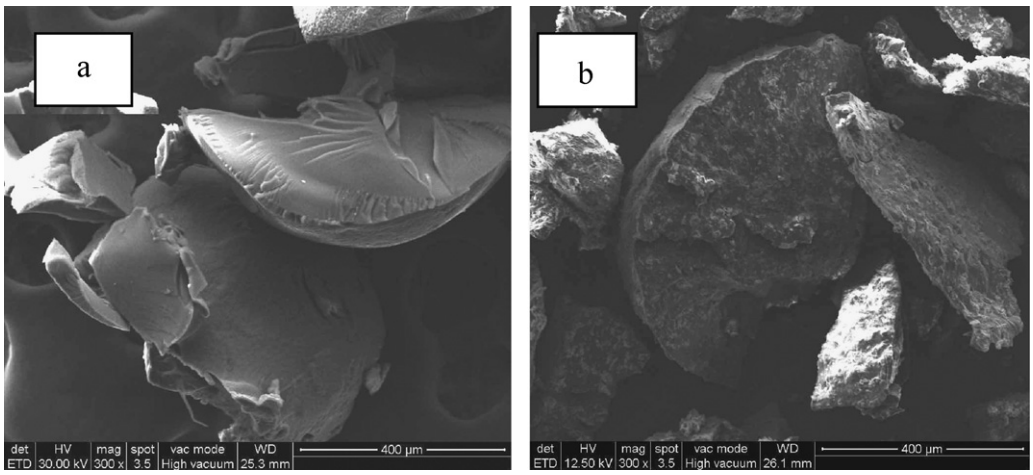

Fig. 1. ESEM images of the cross-linked CS (a) and of the CS/CPL composite (b) in dry state.

the metal solution (mg/L); C_e – equilibrium concentration of the metal solution (mg/L).

The amount of metal ion adsorbed at equilibrium, q_e (mg/g), was calculated by:

$$q_e\,(\mathrm{mg/g}) = \frac{(C_i - C_e)V}{W}, \tag{2}$$

where C_i and C_e are the liquid-phase concentrations of metal ions at initial and equilibrium, respectively; V – the volume of the solution (L); W – the mass of dry sorbent (g).

The adsorption removal efficiency of radiocations from aqueous solution was calculated as follows:

$$\text{removal efficiency}\,(\%) = \frac{C_i - C_f}{C_i} \times 100 \tag{3}$$

where C_f is the final concentration of metal ions.

2.4. Desorption experiments

Desorption is a very important process, both the regeneration of the sorbent and the recovery of metal ions being strongly required in the adsorption experiments. Desorption studies were carried out in batch system using the radioactive ions-loaded CS/CPL composite immediately after the adsorption experiment. Herein, 0.1 M HNO_3, 0.1 M HCl and 0.1 M Na_2CO_3 have been used as desorption agents, desorption time being 6 h in all experiments. The concentration of metal ions in the supernatant has been spectrophotometrically performed, as previously shown in Section 2.3.

Percentage of radiocation desorbed was calculated with Eq. (4):

$$\text{recovered}\,(\%) = \frac{\text{radiocation}_{ads} - \text{radiocation}_{des}}{\text{radiocation}_{ads}} \times 100 \tag{4}$$

where radiocation_{ads} is the amount of radiocation adsorbed onto composite (mg/g), and radiocation_{des} is the amount of radiocation desorbed (mg/g).

3. Results and discussion

The CS/CPL composite microspheres stabilized only by the ionotrop gelation with TPP do not preserve their integrity when they are used in acidic or basic environment. Therefore, the covalent cross-linking with ECH has been used to prepare CS/CPL composites with a high chemical stability. ECH was preferred as a cross-linker because further hydrophilic groups are generated (OH), which could contribute to the increase of the chelating performances of the whole system.

First information on the presence of CPL in the CS/CPL composite was given by ESEM. Typical cross-sectional micrographs of the cross-linked CS beads and of the CS/CPL composite are presented in Fig. 1.

A dense and uniform morphology without pores can be seen in Fig. 1a for the cross-linked CS. The morphology of the CS/CPL composites was different, the presence of CPL being observed as discrete zones in Fig. 2b. The energy dispersive X-ray analysis (EDX) was performed to know the elemental composition of the CS/CPL composite. EDX spectra were consistent with the presence of Al and Si from CPL, and C, N, and O from CS.

The average size of the microspheres in dry state was 800 μm, measured by ESEM. The average size of the composite microspheres in hydrated state was 1200 μm.

The XR diffractograms of cross-linked CS and CPL showed a low crystallinity for the cross-linked CS, and a high degree of crystallinity (χ = 74%) for CPL (Fig. 2).

The crystallinity increased and some definite peaks have been observed in the CS/CPL composite compared with the cross-linked CS, the most intense peaks of CPL: $2\theta = 9.92^\circ$ and 22.5°, respectively for d = 8.90 Å and 3.94 Å, being present in the composite.

FTIR spectra show changes in the structure of CS/CPL composite compared with the cross-linked CS (Fig. 3).

The characteristic bands of CS were located at 1654 cm^{-1}, assigned to the stretching vibrations of the C=O bond in acetamide groups, amide I band, 1562 cm^{-1}, stretching vibration of N–H bond, amide II band, and at 1322 cm^{-1}, characteristic band for the N-acetylglucosamine. The main characteristic bands of CPL were found at the wavelengths of 467 cm^{-1}, 608 cm^{-1}, 795 cm^{-1},

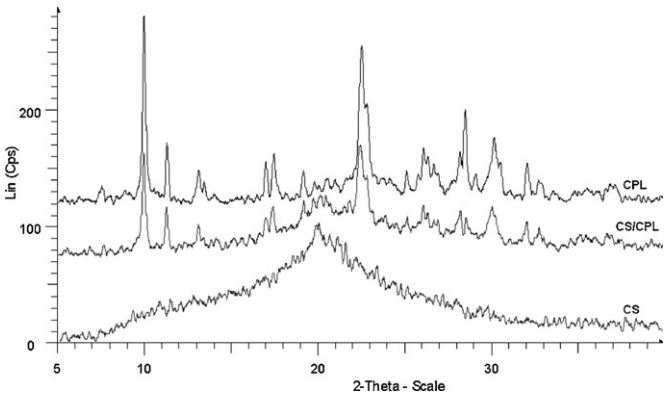

Fig. 2. XR diffractograms of the CPL, cross-linked CS, and CS/CPL composite.

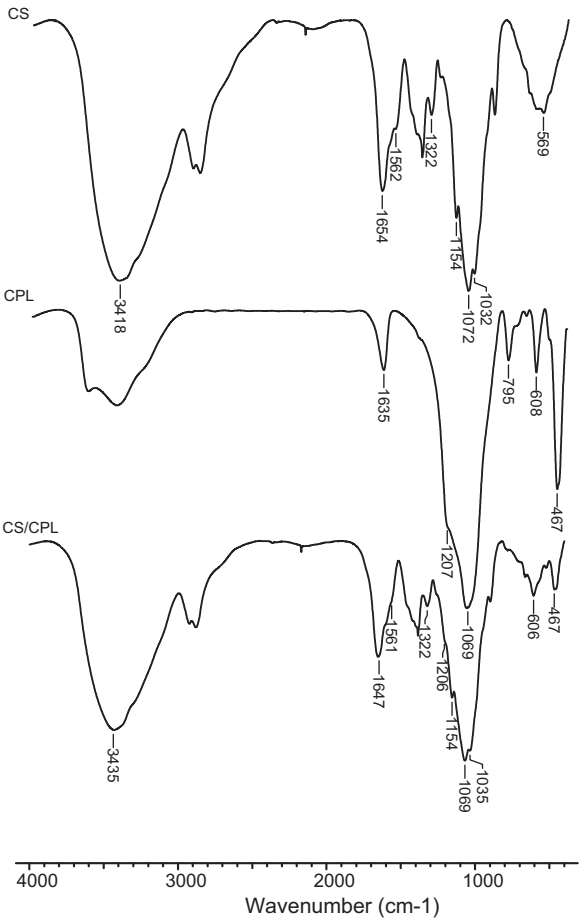

Fig. 3. FTIR spectra of cross-linked chitosan (CS), clinoptilolite (CPL) and CS/CPL composite.

1069 cm^{-1} and 1635 cm^{-1}. The band at 467 cm^{-1} resulted from the stretching vibrations of Al–O bonds, and the bands at 795 cm^{-1} and 1069 cm^{-1} were assigned to Si–O–Si bonds. The peak at 608 cm^{-1}, assigned to the vibration of the external linkage of the tetrahedra, and the peak at 467 cm^{-1} were also observed in the composite CS/CPL. Some of the characteristic bands of CS were either red-shifted, the amide I band was shifted from 1654 cm^{-1}, in cross-linked CS without CPL, to 1647 cm^{-1}, or blue-shifted, the intense band at 3418 cm^{-1} assigned to the stretching vibration of O–H and N–H bonds, as well as to hydrogen bonds, shifted to 3435 cm^{-1} in the CS/CPL composite. The band at 1032 cm^{-1}, assigned to the stretching vibration of the C–O bonds in anhydroglucose ring, diminished in the composite CS/CPL.

The values of surface charge density found by colloidal titration were: (1) cross-linked CS, at pH 4.0, 0.00435 meq/g, and at pH 5.5, 0.00432 meq/g; (2) CS/CPL composite, at pH 4.0, 0.00182 meq/g, and at pH 5.5, 0.0017 meq/g. These values show that at the pH selected for the adsorption experiments the surface charge was very low for both sorbents. The PZC values found for the cross-linked CS and CS/CPL composite were 7.61 and 6.90, respectively. Both the surface charge density and PZC values support the chelation by the free amino groups of CS was the main mechanism of adsorption.

3.1. Kinetic models

Fig. 4 shows the amount of metal ion adsorbed on either cross-linked CS or CS/CPL composite as a function of contact time, at pH 4.0 for UO_2^{2+} and at pH 5.5 for Th^{4+}, at a temperature of 293.15 K,

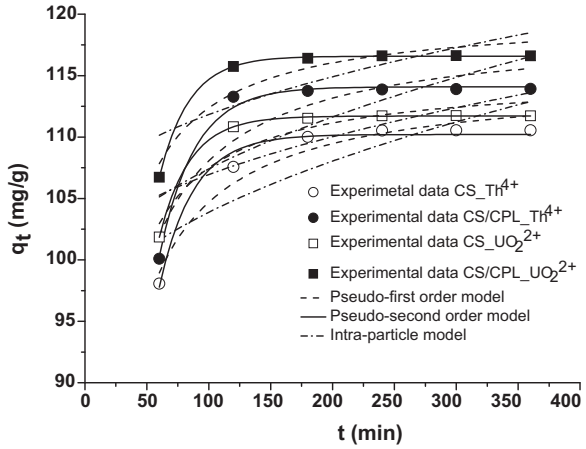

Fig. 4. Plots of q_t vs. t for Th^{4+} and UO_2^{2+} adsorption onto cross-linked CS and CS/CPL composite (initial metal concentration of 20 mg/L, mass of sorbent = 0.04 g).

and a concentration of 20 mg/L. It is obvious that the equilibrium has been established after 180 min for all systems, and that further increase of the contact duration did not influence the sorption process.

In order to investigate the controlling mechanism of adsorption process of cross-linked CS and CS/CPL composite against Th^{4+} and UO_2^{2+} radiocations, three different kinetic models, i.e., the pseudo-first order and pseudo-second order models and the intra-particle diffusion model were used to evaluate the experimental data obtained (Fig. 4).

The constants corresponding to the pseudo-first order and pseudo-second order models and the intra-particle diffusion model were calculated with an Origin 7.5 program by applying Eq. (5) for the pseudo-first order model, Eq. (6) for the pseudo-second order model, and Eq. (7) for the intra-particle diffusion model, the values being presented in Table 1.

$$\log(q_e - q_t) = \log(q_e) - \frac{k_1}{2.303}t \quad (5)$$

$$\frac{t}{q_t} = \frac{1}{k_2 q_e^2} + \frac{1}{q_e}t \quad (6)$$

$$q_t = k_{id}t^{0.5} \quad (7)$$

where q_e and q_t are the amounts of radiocation adsorbed at equilibrium (mg/g) and at time t, respectively, k_1 is the rate constant of pseudo-first order kinetic (min^{-1}), k_2 is the rate constant of pseudo-second order kinetic (g/(mg × min)), and k_{id} is the intra-particle diffusion rate constant (mg/(g × $min^{0.5}$)).

The theoretical $q_{e,calc}$ values estimated from the pseudo-first order model gave significantly different values compared to experimental values, the correlation coefficients being also low (Table 1). These results showed that the pseudo-first order kinetic model did not describe well these sorption systems. The adsorption data were also treated according to the pseudo-second order kinetics (Eq. (6)). As Table 1 shows, the correlation factors are high for the adsorption of Th^{4+} and UO_2^{2+} radiocations onto the cross-linked CS and CS/CPL composite. Moreover, the values of $q_{e,calc}$ estimated from the pseudo-second order model are close to those experimentally found (Table 1). Therefore, it could be suggested that the adsorption of Th^{4+} and UO_2^{2+} radiocations onto the cross-linked CS and CS/CPL composite obeys pseudo-second order model better than pseudo-first order model. The pseudo-second order kinetics supports the chemisorption would be the rate-determining step controlling the adsorption process of metal ion, in agreement with the results reported by other groups [10,18,19,28].

Table 1
Kinetic data for the adsorption of Th^{4+} and UO_2^{2+} on cross-linked CS and CS/CPL composite.

Sorbent	Ions	$q_{e,exp}$ (mg/g)	Pseudo-first order constants			Pseudo-second order constants		Intra-particle diffusion constants		
			$q_{e,calc}$ (mg/g)	k_1 (min^{-1})	R^2	$q_{e,calc}$ (mg/g)	k_2 (g/(mg × min)	R^2	k_{id} (mg/(g × $min^{0.5}$))	R^2
CS	Th^{4+}	110.54	114.693	0.036	0.954	110.21	0.906×10^{-3}	0.983	1.005	0.716
	UO_2^{2+}	111.74	115.07	0.041	0.894	111.71	0.850×10^{-3}	0.999	0.744	0.611
CS/CPL	Th^{4+}	113.92	118.756	0.035	0.861	114.09	1.225×10^{-3}	0.994	1.017	0.575
	UO_2^{2+}	116.62	119.942	0.041	0.894	116.58	1.234×10^{-3}	0.999	0.743	0.61

In order to assess the nature of the diffusion process for the adsorption of metal ions onto the composite, the pore diffusion coefficients were calculated, the values of intra-particle diffusion rate constant, k_{id}, being also presented in Table 1. The deviation of straight lines from the origin indicates that intra-particle transport is not the rate-limiting step, in the adsorption process of Th^{4+} and UO_2^{2+} radiocations onto the CS/CPL composite and cross-linked CS (Fig. 4).

3.2. Effect of initial metal concentration and equilibrium adsorption isotherms

The initial concentration of metal ions is a very important parameter, which influences the sorption process. Therefore, the initial concentration of radiocations in the adsorption process on the cross-linked CS and CS/CPL composite was varied in the range 10–100 mg/L, the other parameters being kept constant (pH 4 for UO_2^{2+}, and 5.5 for Th^{4+}, temperature 293.15 K, contact time 180 min). The adsorption capacity (mg/g) and the removal efficiency (%) as a function of the initial metal concentration are presented in Fig. 5 for Th^{4+}, and in Fig. 6 for UO_2^{2+}.

It is clear that the removal efficiency of radiocations decreased with increasing the initial metal concentration in the aqueous solution, because more mass of radiocations is put into the system with increasing the initial metal concentration in the aqueous solution, the amount of sorbent being the same. On the other hand, because of the higher mobility of Th^{4+} and UO_2^{2+} radiocations in the diluted solutions, the interaction of these ions with the sorbent increases. As can be observed from Figs. 5 and 6, the adsorption capacity of Th^{4+} and UO_2^{2+} radiocations onto the cross-linked CS and CS/CPL composite increased with the increase of the initial metal concentration. This result is similar to that reported by Wang et al. in their study on the adsorption of U(VI) from aqueous solutions using cross-linked CS [19].

It is known that the hydrolysis of uranyl ions plays significant role in determining the equilibrium between U(VI) in solution and on adsorbent [19]. In aqueous solution, uranium exists as U(III), U(IV), U(V) and U(VI). The most important and stable ion in aqueous solution is UO_2^{2+}. The hydrolysis products occur, including $UO_2(OH)^+$, $(UO_2)_2(OH)_2^{2+}$ and $(UO_2)_3(OH)_5^{3+}$, $(UO_2)_2(OH)_2$, their concentrations depending on the value of pH and on the concentration of uranyl ion, which results in decline of adsorption removal efficiency of U(VI) [29,30]. It was reported that the maximum removal efficiency of U(VI) by the cross-linked CS has been located at pH 3–4.5, and after that a slow decline took place with further increase of pH [19]. On the other hand, at pH < 3.0, more protons are available to protonate amine groups, the number of binding sites available for the adsorption of UO_2^{2+} being thus decreased. Th(IV) ions have the highest volume among the tetravalent ions of actinides and are the least hydrolysable. Th(IV) ions can be studied in a large range of concentrations at pH > 4 [30]. The higher retention capacity against UO_2^{2+} compared with Th^{4+} ions could be attributed to the higher level of hydration of Th^{4+} ions in solution, i.e., the adsorption increases with the decrease of the hydrated radiocation radius [29,30].

Analysis of equilibrium data is fundamental in describing how pollutants interact with sorbents, for predicting the adsorption capacity of the adsorbent, which is one of the main parameters required to design an optimized adsorption system [31]. Plot of the solute adsorbed onto the solid surface (mg/g) as a function of the solute concentration in the solution at equilibrium (mg/L), at constant temperature, gives an adsorption isotherm, which can be described by some adsorption models. Fig. 7 shows that the retention capacity of cross-linked CS and CS/CPL composite for Th^{4+} and UO_2^{2+} radiocations increased with the increase of the equilibrium metal concentration resulting in a concave curve, i.e., an isotherm of type L, according to the classification of Limousin et al. [32]. Three isotherm equations have been tested in the present study, namely the Freundlich, Langmuir and Sips isotherm models (Fig. 7).

Freundlich isotherm is the earliest known relationship that describes the surface heterogeneity of the sorbent. It considers multilayer adsorption with a heterogeneous energetic distribu-

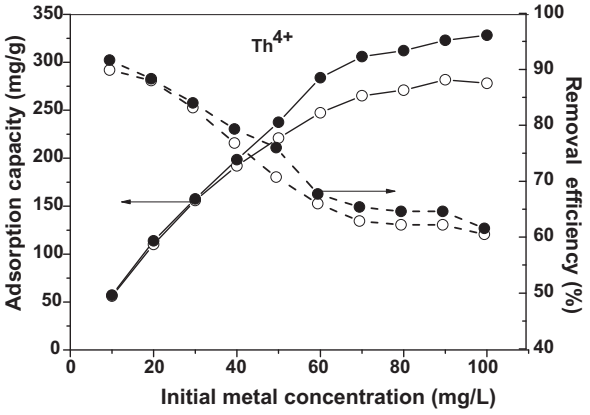

Fig. 5. Effect of initial metal concentration on the adsorption capacity (solid line) and removal efficiency (dash line) of Th^{4+} radiocations onto cross-linked CS (opened circle) and CS/CPL composite (closed circle).

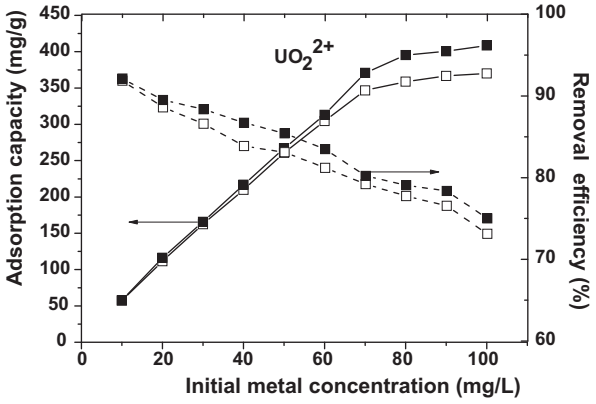

Fig. 6. Effect of initial metal concentration on the adsorption capacity (solid line) and removal efficiency (dash line) of UO_2^{2+} radiocations onto cross-linked CS (opened square) and CS/CPL composite (closed square).

Table 2
Adsorption isotherm constants for Th^{4+} and UO_2^{2+} adsorption onto cross-linked CS and CS/CPL composite.

Sorbent	Ions	Freundlich model				Langmuir model					Sips model				
		K_F (mg/g)	N	R^2	χ^2	K_L (L/mg)	b (mg/g)	R^2	R_L	χ^2	q_m (mg/g)	a_S	N	R^2	χ^2
CS	Th^{4+}	83.93	0.344	0.969	206.93	0.192	314.44	0.991	0.206	57.52	359.33	0.205	0.788	0.996	27.04
	UO_2^{2+}	99.80	0.432	0.941	871.27	0.152	482.66	0.990	0.247	125.07	476.05	0.156	0.745	0.997	118.36
CS/CPL	Th^{4+}	86.084	0.385	0.980	205.51	0.147	385.51	0.991	0.253	84.42	438.55	0.135	0.875	0.993	27.81
	UO_2^{2+}	97.03	0.478	0.962	685.09	0.125	562.58	0.994	0.285	95.94	536.35	0.122	0.921	0.994	116.72

tion of active sites, accompanied by interactions between adsorbed molecules [32]. The non-linear form of Freundlich equation is:

$$q_e = K_F C_e^N \quad (8)$$

where K_F, Freundlich constant, which predicts the quantity of metal ion adsorbed per gram of sorbent at the equilibrium concentration, q_e; N, a measure of the nature and strength of the adsorption process and of the distribution of active sites. If $N < 1$, bond energies increase with the surface density; if $N > 1$, bond energies decrease with the surface density, and when $N = 1$, all surface sites are equivalent.

Langmuir adsorption isotherm, originally developed to describe gas–solid-phase adsorption onto activated carbon, has traditionally been used to quantify the performance of different bio-sorbents [17–19]. This model assumes monolayer coverage of adsorbate onto a homogeneous adsorbent surface. The mathematical expression of Langmuir isotherm model is described by Eq. (9):

$$q_e = \frac{K_L b C_e}{1 + K_L C_e} \quad (9)$$

where q_e is the amount of metal ion adsorbed in mg/g, C_e is the concentration (mg/L) of metal ion in the solution at equilibrium; the Langmuir constants K_L and b represent adsorption equilibrium constant and saturated monolayer adsorption capacity, respectively.

Sips isotherm is a combination of the Langmuir and Freundlich isotherm type models and expected to describe heterogeneous surfaces much better. At low sorbate concentrations it reduces to a Freundlich isotherm, while at high sorbate concentrations it predicts a monolayer adsorption capacity characteristic of the Langmuir isotherm [31]. The Sips isotherm is described by the following equation:

$$q_e = \frac{q_m a_S C_e^N}{1 + a_S C_e^N} \quad (10)$$

where q_m is monolayer adsorption capacity (mg/g) and a_S is Sips constant related to energy of adsorption.

The constants corresponding to the adsorption models were calculated with an Origin 7.5 program by applying Eq. (8) for the Freundlich model, Eq. (9) for the Langmuir model and Eq. (10) for Sips isotherm, and were collected in Table 2.

As Table 2 shows, the experimental data obtained for the adsorption of Th^{4+} and UO_2^{2+} radiocations onto cross-linked CS and CS/CPL composite well fitted in the Langmuir model with a maximum theoretical adsorption capacity of 314.44 mg Th^{4+}/g CS, 482.66 mg UO_2^{2+}/g CS, 385.51 mg Th^{4+}/g CS/CPL composite and 562.58 mg UO_2^{2+}/g CS/CPL composite. According to Sips model, the monolayer adsorption capacity values, q_m, are very close to the maximum theoretical adsorption capacity values, estimated from the Langmuir model (Table 2). Furthermore, the exponent N values for cross-linked CS and CS/CPL composite were closer to unity, which shows that Th^{4+} and UO_2^{2+} radiocations adsorption data are better described by the Langmuir isotherm than by the Freundlich isotherm. The CS/CPL composite showed better retention capacity for both radiocations compared with cross-linked CS. The ability of a material to capture metals is controlled, in part at least, by the number of available functional groups for metal binding [16]. The increase of the adsorption capacity of the CS/CPL composites compared with cross-linked CS could be explained by a synergy of both components, the presence of CPL microparticles leading to the increase of the accessibility at the functional groups of CS network.

According to the values listed in Table 3, the adsorption capacities, found in this work for the radiocations under study, are higher than those reported in literature, and this recommend the novel composite as an alternative for the sorption of Th^{4+} and UO_2^{2+} radiocations.

The essential features of a Langmuir isotherm can be expressed in terms of a dimensionless constant separation factor or equilibrium parameter, R_L (Eq. (11)), which is used to predict if a certain

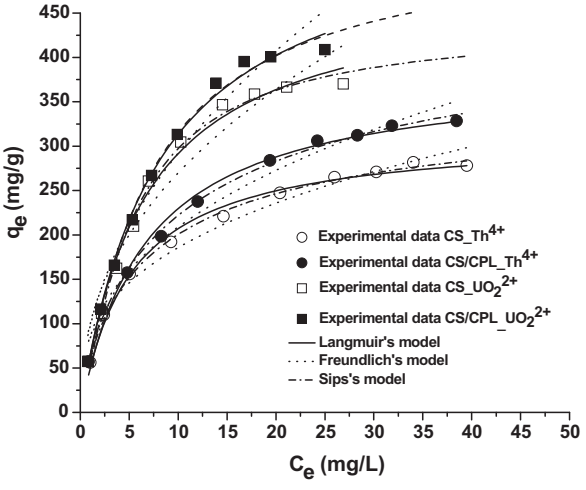

Fig. 7. Comparison of experimental and calculated data for three models for the adsorption of UO_2^{2+} and Th^{4+} onto cross-linked CS and CS/CPL composite. The calculated data were obtained with an Origin 7.5 program by applying Eq. (8) for the Freundlich model, Eq. (9) for the Langmuir model, and Eq. (10) for the Sips model.

Table 3
Comparison of theoretical adsorption capacities (q_{max}, mg/g) for Th^{4+} and UO_2^{2+} of different sorbents.

Sorbent	q_{max} (mg/g)		Reference
	Th^{4+}	UO_2^{2+}	
CS/poly(acrylamide) composite	118.32	72.9	[18]
Cross-linked CS	–	72.46	[19]
Cross-linked CS with 3,4-dihydroxybenzoic acid moiety	–	330.2	[33]
Poly(acrylamide)/apatite composite	294.64	186.3	[34]
CS/perlite composite	–	148.5	[35]
Cross-linked CS beads	359.33	476.05	This study
CS/CPL composite	438.55	536.35	This study

sorbent is "favorable" or "unfavorable" [36].

$$R_L = \frac{1}{1 + K_L C_i} \quad (11)$$

where C_i is the initial metal concentration. The value of R_L indicates as the process to be: unfavorable ($R_L > 1$), linear ($R_L = 1$), favorable ($0 < R_L < 1$) or irreversible ($R_L = 0$). Herein, R_L values obtained for Th^{4+} and UO_2^{2+} ions are listed in Table 2. The fact that all the R_L values for the adsorption of Th^{4+} and UO_2^{2+} radiocations onto the cross-linked CS and CS/CPL composite are in the ranges of 0–1 for 20 mg/L initial metal concentration, confirmed that these sorbents are favorable for the adsorption of Th^{4+} and UO_2^{2+} radiocations under the selected conditions (Table 2).

3.3. Statistics analysis

Determining the best-fitting model is a key analysis to mathematically describe the involved sorption system and, therefore, to explore the related theoretical assumptions. Hence, several error calculation functions have been widely used to estimate the error deviations between experimental and theoretically predicted equilibrium adsorption values, including the average relative error deviation, the Marquardt's percent standard error deviation, the hybrid fractional error function, the non-linear Chi-square test (χ^2), the correlation coefficient of determination (R^2), Spearman's correlation coefficient, the standard deviation of relative errors, etc. [31]. In this study, two statistical functions are analysed to investigate their applicability as suitable tools to evaluate isotherm models fitness, namely the correlation coefficient of determination (R^2) and the non-linear χ^2 test. The χ^2 test statistic is basically the sum of the squares of the differences between the experimental data and the data obtained by calculating from models, with each squared difference divided by the corresponding data calculated using the models. This can be represented mathematically as:

$$\chi^2 = \sum \frac{(q_{e,exp} - q_{e,cal})^2}{q_{e,cal}} \quad (12)$$

where $q_{e,cal}$ is the equilibrium capacity obtained by calculating from the model (mg/g) and $q_{e,exp}$ is the experimental data of the equilibrium capacity (mg/g). If data from a model are similar to the experimental data, χ^2 will be a small number, and if they differ, χ^2 will be a big number [18,31].

The results of the application of correlation coefficients (R^2) and non-linear χ^2 test on experimental data of the equilibrium capacity for the three adsorption isotherms are shown in Table 2. The Sips isotherm model appears to be the best fitting model for radiocations adsorption onto the cross-linked CS and CS/CPL composite, with the highest correlation coefficient ($R^2 = 0.995$) and the lowest χ^2 value (Table 2). Even though the Langmuir isotherm model has also high correlation coefficient ($R^2 = 0.991$) for radiocations adsorption onto the cross-linked CS and CS/CPL composite, the high χ^2 values (Table 2) indicate that adsorption of radiocations onto the cross-linked CS and CS/CPL composite is not homogeneous. Table 2 shows that the Freundlich isotherm model has the lowest correlation coefficients and the highest χ^2 values for all the adsorbents used in this study.

3.4. Effect of sorbent mass

The effect of the sorbent amount on the distribution coefficient, K_d, was studied at a concentration of radiocation of 50 mg/L, and at a temperature of 293.15 K, pH being the same in all experiments (4.0 in the case of UO_2^{2+}, and 5.5 in the case of Th^{4+}). Fig. 8 shows that K_d monotonously increased with the increase of the sorbent mass from 0.01 up to 0.04 g, a higher mass of sorbent having a higher number of active centres on the surface, available for the sorption of metal ions.

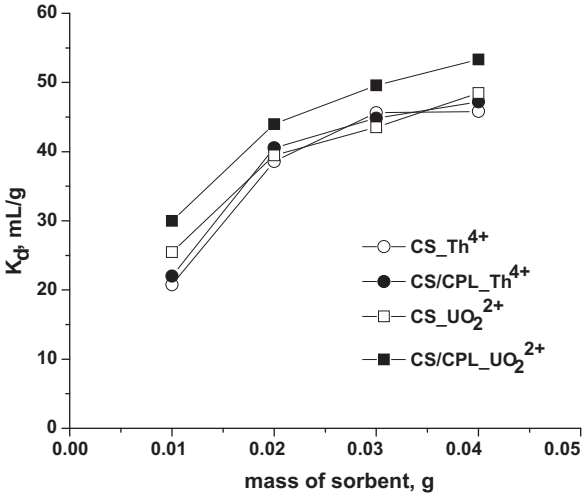

Fig. 8. Th^{4+} and UO_2^{2+} ions retention as a function of sorbent mass at an initial radionuclide concentration of 50 mg/L, and a temperature of 293.15 K.

3.5. Effect of temperature and thermodynamic data

The effect of temperature on the sorption of radioactive ions on the cross-linked CS and CS/CPL composite has been investigated at 293.15, 303.15, 313.15, 323.15 and 333.15 K, the values of K_d as a function of temperature being plotted in Fig. 9.

As Fig. 9 shows the sorption capacities reinforced with the rise of temperature indicating the process is endothermic, and this could be attributed, mainly, to the increase of the nonelectrostatic interactions. The increase of the sorption capacity of uranyl ions on the chitosan/attapulgite composite, with the increase of temperature, has been also reported [37].

The thermodynamic parameters, such as: standard enthalpy (ΔH°) and standard entropy (ΔS°) were calculated from the slopes and intercepts of the linear variation of $\ln K_d$ *vs.* $1/T$ (Fig. 10), with Eq. (13):

$$\ln K_d = \frac{\Delta S^\circ}{R} - \frac{\Delta H^\circ}{RT} \quad (13)$$

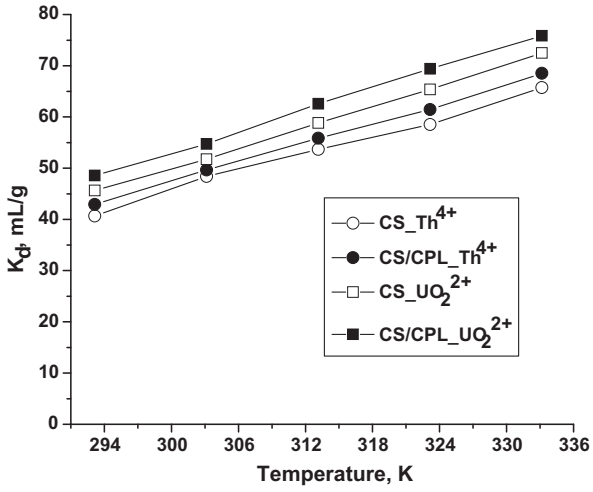

Fig. 9. Effect of temperature on the adsorption of Th^{4+} and UO_2^{2+} by the cross-linked CS and CS/CPL composite at an initial concentration of metal ions of 20 mg/L.

Table 4
Thermodynamic parameters for the sorption of Th^{4+} and UO_2^{2+} onto cross-linked CS and CS/CPL composite.

Ions	Sorbent	ΔH° (J/mol)	ΔS° (J/mol K)	ΔG° (kJ/mol)				
				293.15 K	303.15 K	313.15 K	323.15 K	333.15 K
Th^{4+}	CS	8.81	34.75	−10.17	−10.52	−10.77	−11.22	−11.56
	CS/CPL	8.88	35.08	−10.24	−10.62	−10.97	−11.32	−11.67
UO_2^{2+}	CS	9.06	35.58	−10.42	−10.77	−11.13	−11.48	−11.84
	CS/CPL	9.67	35.91	−10.51	−11.87	−11.23	−11.59	−11.95

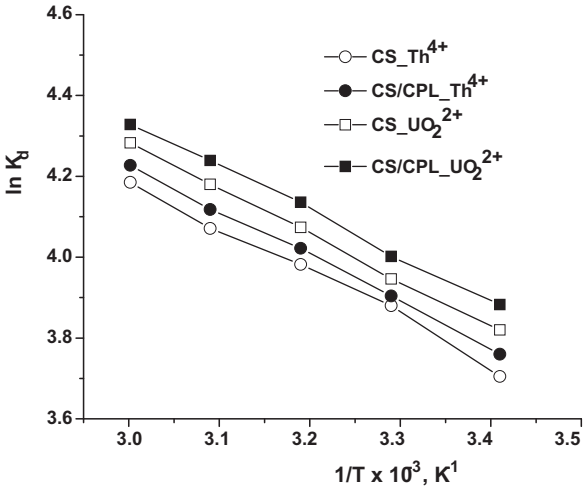

Fig. 10. Relation between $\ln K_d$ and sorption temperature.

where K_d is the distribution coefficient, T is absolute temperature (K), and R is the ideal gas constant (8.314 kJ/mol K).

The Gibbs free energy values were calculated by Eq. (14):

$$\Delta G^\circ = \Delta H^\circ - T\Delta S^\circ \quad (14)$$

The obtained thermodynamic parameters from Eqs. (13) and (14) are presented in Table 4.

The positive values of ΔH° indicates that the sorption process is endotherm in nature [36,37]. The negative values of Gibbs free energy indicates a spontaneous sorption process, and the decrease of this parameter with the increase of temperature shows the sorption is more efficient at higher temperatures. The positive values of ΔS° reflect the affinity of the CS/CPL beads for radiocations and suggests the increased randomness at the solid–solution interface during adsorption.

3.6. Competitive adsorption of uranyl and thorium cations

To check if the CS/CPL composite can be useful for selective separation of metal cations, sorption studies were performed under competitive conditions, i.e., using binary and quaternary mixtures of UO_2^{2+} or Th^{4+} with Cu^{2+}, Fe^{2+} and Al^{3+}. The obtained results as adsorbed amount of each cation are summarized in Table 5.

As Table 5 shows, the presence of Al^{3+} cations leads to the lowest sorption amounts, in binary systems, for both UO_2^{2+} or Th^{4+} radiocations. It can be also observed that the retention capacity for all cations decreases in quaternary system. The overall adsorption tendency of CS/CPL composite toward UO_2^{2+} and Th^{4+} radiocations, under competitive conditions, followed the order: $Cu^{2+} > UO_2^{2+} > Fe^{2+} > Al^{3+}$, and $Cu^{2+} > Th^{4+} > Fe^{2+} > Al^{3+}$, respectively. The adsorption of uranyl ions under competitive conditions, in presence of Pb(II), Cu(II) and Ni(II) on ACSD (alginate coated sepiolite and calcined diatomite earth) showed the following series: $Pb^{2+} \gg Cu^{2+} > Ni^{2+} > UO_2^{2+}$, i.e., the lowest adsorption capacity has been found for uranyl ions [38].

Table 6
Effects of some eluents on Th^{4+} and UO_2^{2+} desorption.

Radiocations	Sorbent	desorption (%)		
		0.1 M HCl	0.1 M HNO_3	0.1 M Na_2CO_3
Th^{4+}	CS	82.64	68.79	62.4
	CS/CPL	85.41	71.65	64.84
UO_2^{2+}	CS	76.52	82.63	89.54
	CS/CPL	78.25	88.25	92.43

3.7. Desorption studies

The data obtained from the desorption experiments are presented in Table 6.

The desorption level of UO_2^{2+} from the composite CS/CPL, by using 0.1 M Na_2CO_3, was around 92%, and that of Th^{4+} ions, performed by 0.1 M HCl, was around 85%, both values being higher than the desorption level of radiocations from the cross-linked CS, which were 89% and 83%, respectively. Thus, the results of desorption tests show that the sorption process is reversible and also the possibility to reuse the composite sorbent taking into account the high recovery level of both radiocations.

Table 5
Adsorption capacity of metal ions under competitive conditions.

Metal Ions	Adsorbed metal (mg/g)			
	UO_2^{2+}–Cu^{2+}	UO_2^{2+}–Fe^{2+}	UO_2^{2+}–Al^{3+}	UO_2^{2+}–Cu^{2+}–Fe^{2+}–Al^{3+}
UO_2^{2+}	385.43	382.15	373.4	358.35
Cu^{2+}	425.21	–	–	397.21
Fe^{2+}	–	354.85	–	321.48
Al^{3+}	–	–	278.34	253.67
	Th^{4+}–Cu^{2+}	Th^{4+}–Fe^{2+}	Th^{4+}–Al^{3+}	Th^{4+}–Cu^{2+}–Fe^{2+}–Al^{3+}
Th^{4+}	315.42	312.73	302.63	298.32
Cu^{2+}	393.72	–	–	371.23
Fe^{2+}	–	272.7	–	265.42
Al^{3+}	–	–	257.3	250.43

4. Conclusions

The sorption of UO_2^{2+} and Th^{4+} ions from simulated radioactive solutions onto the CS/CPL composite and cross-linked CS has been studied as a function of contact time, initial metal ion concentration, sorbent mass and temperature. The adsorption process of both radiocations obeyed of the pseudo-second order kinetics, supporting the chemisorption would be the rate-determining step.

The equilibrium data obtained for the adsorption of radiocations onto the CS/CPL composite well fitted in the Sips model with a maximum theoretical adsorption capacity of 438.55 mg Th^{4+}/g composite, and 536.35 mg UO_2^{2+}/g composite, the adsorption capacity being higher for both radiocations compared with the cross-linked CS. The higher retention capacity against UO_2^{2+} compared with Th^{4+} ions could be attributed to the higher level of hydration of Th^{4+} ions in solution, i.e., the adsorption increasing with the decrease of the hydrated radiocation radius. Under competitive conditions, the adsorption tendency of CS/CPL composite toward UO_2^{2+} and Th^{4+} radiocations followed the order: $Cu^{2+} > UO_2^{2+} > Fe^{2+} > Al^{3+}$, and $Cu^{2+} > Th^{4+} > Fe^{2+} > Al^{3+}$.

The adsorption process was spontaneous ($\Delta G^\circ < 0$) and endothermic ($\Delta H^\circ > 0$). The results obtained in the desorption process indicated 0.1 M Na_2CO_3 as the best desorption agent for the UO_2^{2+} ions, while for the desorption of the Th^{4+} ions, the best results were obtained with 0.1 M HCl solution.

Acknowledgements

This work was supported by CNCSIS-UEFISCSU, project No. PNII-IDEI ID_405/2007, and by the project PNII-IDEI ID_981/2008.

References

[1] M.A. Hanif, R. Nadeem, H.N. Bhatti, N.R. Ahmad, T.M. Ansari, Ni(II) biosorption by *Cassia fistula* (Golden Shower) biomass, J. Hazard. Mater. B139 (2007) 345–355.
[2] D. Satapathy, G.S. Natarajan, Potassium bromate modification of granular activated carbon and its effect on nickel adsorption, Adsorption 12 (2006) 147–154.
[3] X. Wang, S. Xia, L. Chen, J. Zhao, J. Chovelon, J. Nicole, Biosorption of cadmium(II) and lead(II) ions from aqueous solutions onto dried activated sludge, J. Environ. Sci. 18 (2006) 840–844.
[4] E. Popovici, D. Humelnicu, C. Hristodor, Removal of UO_2^{2+} ions from simulated wastewater onto Romanian aluminium pillared clays, Rev. Chim. Bucharest 57 (2006) 675–678.
[5] D. Humelnicu, E. Popovici, C. Mita, E. Dvininov, Study on the retention of uranyl ions on modiffied clays with titanium oxide, J. Radioanal. Nucl. Chem. 279 (2009) 131–136.
[6] T. Tsuruta, Removal and recovery of uranyl ion using various microorganisms, J. Biosci. Bioeng. 94 (2002) 23–28.
[7] H.H. Someda, R.R. Sheha, Solid phase extractive preconcentration of some actinide elements using impregnated carbon, Radiochemistry 50 (2008) 56–63.
[8] D. Bontea, C. Mita, D. Humelnicu, Characterisation of processes occuring during removal of uranyl ions from wastewaters using cellulose and modified cellulose materials, J. Radioanal. Nucl. Chem. 268 (2006) 305–311.
[9] S. Akyil, M.A.A. Aslani, M. Eral, Adsorption characteristics of uranium onto composite ion exchangers, J. Radioanal. Nucl. Chem. 256 (2003) 45–51.
[10] S. Aytas, S. Akyil, M. Eral, Adsorption and thermodynamic behavior of uranium on zeolite, J. Radioanal. Nucl. Chem. 260 (2004) 119–125.
[11] H. Bedelean, M. Stanca, A. Măicăneanu, S. Burcam, Zeolitic volcanic tuffs from Măcicaş (Cluj County), natural raw materials used for NH^{4+} removal from wastewaters, Stud. Univ. Babes-Bolyai, Geologia 52 (2006) 43–49.
[12] M.E. Argun, Use of clinoptilolite for the removal of nickel ions from water: Kinetics and thermodynamics, J. Hazard. Mater. 150 (2008) 587–595.
[13] W. Qiu, Y. Zheng, Removal of lead, copper, nickel, cobalt, and zinc from water by a cancrinite-type zeolite synthesized from fly ash, Chem. Eng. J. 145 (2009) 483–488.
[14] P.R. Shukla, S. Wang, H.M. Ang, M.O. Tadé, Synthesis, characterisation, and adsorption evaluation of carbon-natural-zeolite composites, Adv. Powder Technol. 20 (2009) 245–250.
[15] G. Crini, Recent developments in polysaccharide-based materials used as adsorbents in wastewater treatment, Prog. Polym. Sci. 30 (2005) 38–70.
[16] E. Guibal, Interactions of metal ions with chitosan-based sorbents: a review, Sep. Purif. Technol. 38 (2004) 43–74.
[17] A.-H. Chen, S.-C. Liu, C.-Y. Chen, C.-Y. Chen, Comparative adsorption of Cu(II), Zn(II), and Pb(II) ions in aqueous solution on the crosslinked chitosan with epichlorohydrin, J. Hazard. Mater. 154 (2008) 184–191.
[18] R. Akkaya, U. Ulusoy, Adsorptive features of chitosan entrapped in polyacrylamide hydrogel for Pb^{2+}, UO_2^{2+}, and Th^{4+}, J. Hazard. Mater. 151 (2008) 380–388.
[19] G. Wang, J. Liu, X. Wang, Z. Xie, N. Deng, Adsorption of uranium (VI) from aqueous solution onto cross-linked chitosan, J. Hazard. Mater. 168 (2009) 1053–1058.
[20] E.S. Drăgan, M.V. Dinu, Removal of copper ions from aqueous solution by adsorption on ionic hybrids based on chitosan and clinoptilolite, Ion Ex. Lett. 2 (2009) 15–18.
[21] E.S. Drăgan, M.V. Dinu, D. Timpu, Preparation and characterization of novel composites based on chitosan and clinoptilolite with enhanced adsorption properties for Cu^{2+}, Bioresour. Technol. 101 (2010) 812–817.
[22] M.V. Dinu, E.S. Drăgan, Evaluation of Cu^{2+}, Co^{2+} and Ni^{2+} ions removal from aqueous solution using a novel chitosan/clinoptilolite composite. Kinetics and isotherms, Chem. Eng. J. 160 (2010) 157–163.
[23] X.L. Tan, X.K. Wang, M. Fang, C.L. Chen, Sorption and desorption of Th(IV) on nanoparticles of anatase studied by batch and spectroscopic methods, Colloids Surf. A 296 (2007) 109–116.
[24] D. Humelnicu, L. Bulgariu, M. Macoveanu, On the retention of uranyl and thorium ions from radioactive solutions on peat moss, J. Hazard. Mater. 174 (2010) 782–787.
[25] M.H. Khan, A. Ali, N.N. Khan, Spectrophotometric determination of thorium with disodium salt of Arsenazo III in perchloric acid, J. Radioanal. Nucl. Chem. 250 (2001) 353–357.
[26] A. Kilincarslan, S. Akyil, Uranium adsorption characteristic and thermodynamic behavior of clinoptilolite zeolite, J. Radioanal. Nucl. Chem. 264 (2005) 541–548.
[27] D.A. Kulik, Sorption modelling by Gibbs energy minimisation: Towards a uniform thermodynamic database for surface complexes of radionuclides, Radiochim. Acta 90 (2002) 815–832.
[28] Y.S. Ho, Second-order kinetic model for the sorption of cadmium onto tree fern: a comparison of linear and non-linear methods, Water Res. 40 (2006) 119–125.
[29] N. Mikami, M. Sasaki, K. Hachiya, T. Yasunaga, Kinetic study of the adsorption-desorption of uranyl ion on a γ-Al_2O_3 surface using the pressure jump technique, J. Phys. Chem. 87 (1983) 5478–5481.
[30] F.A. Cotton, G. Wilkinson, C.A. Murillo, M. Bochmann, Advanced Inorganic Chemistry, sixth ed., John Wiley &Sons, Inc., New York, 1999.
[31] K.F. Foo, B.H. Hameed, Insights into the modeling of adsorption isotherm systems, Chem. Eng. J. 156 (2010) 2–10.
[32] G. Limousin, J.-P. Gaudet, L. Charlet, S. Szenknect, V. Barthes, M. Krimissa, Sorption isotherms: a review on physical bases, modeling and measurement, Appl. Geochem. 22 (2007) 249–275.
[33] A. Sabarudin, M. Oshima, T. Takayanagi, L. Hakim, K. Oshita, Y. Hua Gao, S. Motomizu, Functionalization of chitosan with 3,4-dihydroxybenzoic acid for the adsorption/collection of uranium in water samples and its determination by inductively coupled plasma-mass spectrometry, Anal. Chim. Acta 581 (2007) 214–220.
[34] U. Ulusoy, R. Akkaya, Adsorptive features of polyacrylamide–apatite composite for Pb^{2+}, UO_2^{2+} and Th^{4+}, J. Hazard. Mater. 163 (2009) 98–108.
[35] S. Hasan, T.K. Ghosh, M.A. Prelas, D.S. Viswanath, V.M. Boddu, Adsorption of uranium on a novel bioadsorbent-chitosan-coated perlite, Nucl. Technol. 159 (2007) 59–71.
[36] G. Bayramoglu, B. Altintas, M.Y. Arica, Adsorption kinetics and thermodynamic parameters of cationic dyes from aqueous solutions by using a new strong cation exchange resin, Chem. Eng. J. 152 (2009) 339–346.
[37] C. Pang, Y. Liu, X. Cao, R. Hua, C. Wang, C. Li, Adsorptive removal of uranium from aqueous solution using chitosan-coated attapulgite, J. Radioanal. Nucl. Chem., doi:10.1007/s10967-010r-r0635-0.
[38] R. Donat, G.K. Cilgi, S. Aytas, H. Cetisli, Thermodynamic parameters and sorption of U(VI) on ACSD, J. Radioanal. Nucl. Chem. 279 (2009) 271–280.